

## Plug and Play Parallel Transmission at 7 and 9.4 Tesla based on Principles from MR Fingerprinting

Martijn A Cloos<sup>1</sup>, Christopher Wiggins<sup>2</sup>, Graham Wiggins<sup>1</sup>, and Dan Sodickson<sup>1</sup>

<sup>1</sup>NYU Langone Medical Center, New York, NY, United States, <sup>2</sup>Scannexus, Maastricht, Netherlands

**Purpose:** Parallel transmission (PTX)<sup>1,2</sup> is often proposed as a framework for transmit non-uniformity mitigation in ultra high field MRI ( $\geq 7$  Tesla)<sup>3,4</sup>. However, routine application of PTX has hitherto been hampered by technical challenges. In particular, optimal performance is contingent on high quality subject-specific transmit-sensitivity ( $B_1^+$ ) maps. Despite major advances in  $B_1^+$  mapping<sup>5,6</sup>, the necessary calibration scans still impose a significant time penalty on each PTX exam. Moreover, tailored pulse design, needed to achieve high fidelity excitations covering an extended region of interest, remains a computationally demanding and technically challenging endeavor impeding workflow by adding additional delay times between scans. In this work we demonstrate a novel approach to transmit non-uniformity mitigation inspired by the recently proposed MR Fingerprinting (MRF) method<sup>7</sup>.

**Theory:** When image data are acquired in quick succession, the time course of the signal can be matched to a pre-calculated library of simulated spin evolutions. As demonstrated by Ma, et al<sup>7</sup>, when using a suitable encoding scheme, finding the optimal match can reveal quantitative information about the underlying tissue properties. Extending the parameter space covered by the library enables the simultaneous quantification of the  $B_1^+$  field. However, the signal level obtained from areas with extremely low  $B_1^+$  remains compromised. To secure adequate signal throughout the field of view, we have interleaved the individual transmit channels during the encoding of the MR fingerprint. Not only does this circumvent RF-interference effects between coils, which could result in signal voids or Specific Absorption Rate (SAR) hotspots, it also serves to reduce the coherence between reconstruction artifacts and enables the identification of the underlying  $B_1^+$  components corresponding to each of the transmit-channels. Spoiler gradients were inserted to decouple the transmit-phases between channels allowing the reconstruction to focus on the longitudinal relaxation (T1), each of the  $B_1^+$  and relative receive sensitivities ( $B_1^-$ ), as well as a Proton Density or T2-star weighted image.

**Methods:** Experimental validation was performed on Magnetom 7T and 9.4T MRI systems each equipped with 8 channel PTX capability (Siemens, Erlangen, Germany). In this initial demonstration only 4 transmit channels were used (Fig. 1). To this end, the upper 4 channels of a triangular array<sup>8</sup> at 7T and a dual-row transmit array<sup>9</sup> at 9.4T were used. A balanced energy distribution among coils is desired to ensure an even illumination of the field of view and prevent formation of SAR hot spots. This was achieved by concatenating (twice) the ordered set of 4-tuples, resulting in 384 snapshots of the spin evolution (Fig. 2). To further increase the dynamic range, the transmit voltages on individual channels were pseudo-randomly modulated between 0.25 and 1. Imaging parameters (at 7T/9.4T) were 3x3/2x2mm in-plane resolution, 5/2mm slice, TR=40/40ms, TE=19/15ms, Echo Planar Imaging (EPI) readout, total scan time 15s. The library of simulations was constructed using in-house developed software based on the formalism described by Benoit-Cattin, et al<sup>10</sup>. The gradient ascent algorithm was used to quickly find the best matching fingerprint based on the correlation. Once the optimal match was found, the relative  $B_1^+$  profiles were retrieved by calculating the scaling factor with the simulated fingerprint as observed by each receiver. Similarly, the same procedure was applied to the combined data to retrieve a T2 star weighted image. The reconstructed  $B_1^+$  maps were validated against the well-established Actual Flip-Angle Imaging method (AFI, TR1/TR2=40/200, TE=4.5ms, total scan time ~10min)<sup>5</sup>. For validation, the circularly polarized mode (using all 8 channels) was used to create a T1 map based on a series of Inversion Recovery Turbo Spin Echo (IRTSE) images (TI={0.05,0.1,1,2,9s}, TR=10s, TE=12ms, Turbo Factor 5, iPAT 2, 1.65x1.65mm, 5mm slice, total scan time ~15min). A 16cm diameter two-compartment phantom (0.5g NaCl per 750cl H<sub>2</sub>O, doped with 0.5ml or 1.0ml gadolinium) phantom was used for in-vitro validation. In-vivo data were acquired in the human brain at 7T and 9.4T in accordance with the IRB of the relevant institutions.

**Results:** The  $B_1^+$  maps measured in the phantom all demonstrated a correlation above 0.93 (0.95±0.01) with their AFI counterparts. Phantom T1 values (compartment 1 / compartment 2) were; 775±38 / 312±27 vs 756±15 / 346±10 for the proposed and the traditional IRTSE-based method, respectively. The top part of Fig. 3 shows the series of IRTSE images and a zoomed section of the reconstructed T1-map at 7T. The bottom part shows two fingerprints associated with the approximate locations A and B in the zoomed images (Fig. 3). Throughout the brain the optimal matches resulted in correlation factors above 0.99. The T1 values measured with the proposed approach were in excellent agreement with existing literature values (A=1.2s, B=4.4s)<sup>11</sup>. On the other hand, the IRTSE based maps appear to underestimate the T1 in the spinal fluid. The in-vivo measured  $B_1^+$  maps also showed excellent agreement (correlation factor of 0.96±0.01) with the AFI measurements (Fig. 4). At 9.4T, where the IRTSE was compromised by the transmit voltage and SAR limitations (on top of the expected increase in  $B_1^+$  non-uniformity), the proposed approach retained high-quality quantitative information (Fig. 5).

**Discussion:** The simultaneous quantification of both T1 and multiple  $B_1^+$  maps within a scan time of only 15s was demonstrated. Apart from the inherent robustness to subject motion in an MRF-type experiment<sup>7</sup>, the reduced scan time by over one order in magnitude compared to the IRTSE offer practical advantages when scanning a less compliant subject. Admittedly, at the expense of increased SAR, the IRTSE could be run in an interleaved multi-slice fashion. Nonetheless, even when acquiring 40 slices the proposed approach would still be 50% faster. Moreover, the proposed approach does not rely on high-fidelity inversion or refocusing pulses, nor does the SAR increase with the number of slices. Consequently, the energy deposition is reduced substantially due to the lower flip-angles involved, and omission of energy demanding  $B_1^+$  insensitive RF-pulse solutions. Application of this calibration free PTX framework to other parts of the body requires better resilience against chemical shift and off-resonance effects than is possible with the EPI acquisition used in this work. To this end we are currently exploring spiral-based readout trajectories with an incremental golden angle in plane rotation to minimize the coherence of these artifacts in the fingerprint. To enable the simultaneous quantification of T2, we plan to explore a selective spoiling scheme to decouple the relative transmit-phases.

**Conclusion:** A novel approach to excitation non-uniformity mitigation at UHF was demonstrated that utilizes the PTX setup without the need for cumbersome calibration scans or tailored pulse design. It enables fast simultaneous quantitative mapping of the T1 relaxation time and an array of transmit sensitivity profiles in less than 15s.

**References:** <sup>1</sup>Katscher, et al., MRM; 49:144 (2003). <sup>2</sup>Zhu, MRM; 51:755 (2004). <sup>3</sup>Setsompop, et al., MRM; 60:1422

<sup>5</sup>Yarnykh, MRM; 57:92 (2007). <sup>6</sup>Nehrke, et al., MRM; 68:1517 (2012). <sup>7</sup>MA, et al., Nature; 495:187 (2013). <sup>8</sup>Wiggins et al., ISMRM p (2012). <sup>9</sup>Shajan, et al., MRM; Early View (2013). <sup>10</sup>Benoit-Cattin, et al., JMR; 173:96 (2005). <sup>11</sup>Rooney, et al., MRM; 52: 208 (2007).

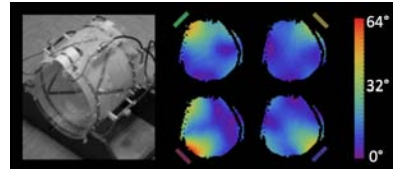


**Figure 1.** Triangular transceiver-array<sup>8</sup>, and transmit sensitivity profiles corresponding to the elements used in the experiments.  $B_1^+$ maps to the right were acquired using AFI<sup>5</sup>.

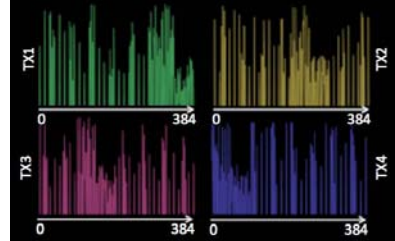


**Figure 2.** Different RF-pulse amplitudes played on each of the channels throughout the acquisition of a single slice. Channel color-coding is in accordance with Fig. 1.

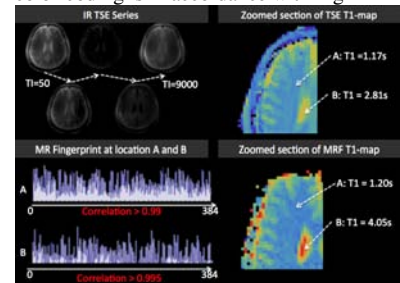


**Figure 3.** Quantitative comparison of IRTSE- and MR-PTX-fingerprinting-based T1 maps at 7T.

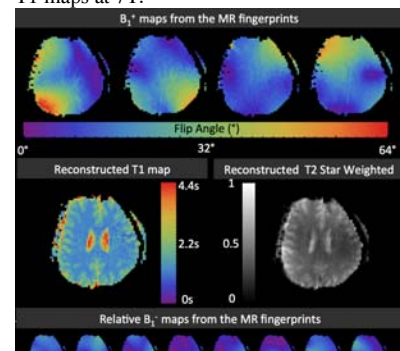


**Figure 4.** Reconstructed  $B_1^+$  maps, T1 map, T2-star image and relative  $B_1^-$  maps derived from a single 15s acquisition.

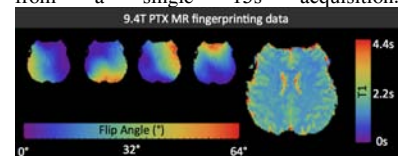


**Figure 5.** Reconstructed  $B_1^+$  maps and T1 map using the PTX MRF method at 9.4T. (2008). <sup>4</sup>Cloos, et al., MRM; 67:72 (2012).